Wang Lisha (Orcid ID: 0009-0003-7739-5354)

Yang Rong (Orcid ID: 0000-0002-2848-5156)

Cultivation increased soil potential denitrification rates by modifying denitrifier communities in desert-oasis ecotone

Lisha Wang[1,2,3], Zhibin He [2*], Chuan Wang[1,3], Longfei Chen[2], Rong Yang[2]

[1] College of Resource Environment and Tourism，Hubei University of Arts and Science，Xiangyang 441053，China

[2] Linze Inland River Basin Research Station, Chinese Ecosystem Research Network, Key Laboratory of Eco-hydrology of Inland River Basin, Northwest Institute of Eco-Environment and Resources, Chinese Academy of Sciences, Lanzhou 730000, China

[3] University of Chinese Academy of Sciences, Beijing 100049, China

[*] Correspondence: hzbmail@lzb.ac.cn Tel：+8613639366653

Abstract

Oases soils in northwestern China are widely used for agricultural production, but low soil moisture and fertility necessitate high volumes of irrigation and fertilization, with significant losses of water via evaporation and nitrogen via denitrification. The dynamics of denitrifying communities and their responses to potential denitrification rate (PDR) in continuously-irrigated oases remain unclear. In this study, we examined the dynamics of nirK and nirS denitrifying communities in three distinct areas: an old oasis field (OOF, 54 years of cultivation), a young oasis field (YOF, 20 years), and an adjacent uncultivated sandy land (USL, 0 years), and used the partial least squares path model (PLS-PM) to predict how and to what extent soil properties and denitrifying communities may be responsible for changes in PDR. Our findings indicate that cultivation, compared to the USL treatment, improved soil structure and fertility, increased the abundance and diversity of denitrifying microbes, resulting in a further elevation of soil PDR in YOF and OOF. Additionally, our analysis highlights the potential dominance of the nirK gene in denitrification. PLS-PM revealed that soil chemical properties and microbial biomass indirectly affected soil PDR by regulating

This article has been accepted for publication and undergone full peer review but has not been through the copyediting, typesetting, pagination and proofreading process which may lead to differences between this version and the Version of Record. Please cite this article as doi: 10.1111/ejss.13425

the abundance and diversity of *nirK* and *nirS* genes. Conversely, soil physical properties had a direct negative impact on PDR. Alterations in PDR were, in part, attributed to changes in abundance, richness, and beta-diversity, but not correlated with changes in alpha-diversity. Notably, the standardized total effect demonstrated that the denitrifier community exhibited greater responsiveness to changes in PDR than did soil properties. Overall, our findings suggest that the denitrifying communities may play a more important role than soil properties in PDR and an increased understanding of the denitrifying communities allows PDR prediction during conversion of oasis to cultivated land conversion.

Keywords: Cultivation; Denitrification rate; Denitrifying community; Desert-oasis region; Illumina Miseq sequencing

1. Introduction

The oasis area in northwest China has grown from 2.5×10^4 km^2 to 12.8×10^4 km^2 since the 1950s due to ongoing agricultural land development (Xue et al., 2019). The change in land use brought on by the development of oases into desert fully changing atmosphere–water–soil–plant system processes in arid regions.

Cultivation, irrigation, and fertilization accelerate soil development processes. Changes in soil properties impact the management of fertilizer and water. Conversion of native desert soil to an irrigated field changes edaphic properties and agricultural practices, and can affect soil microorganisms (Szukics et al., 2009; Attard et al., 2011; Chen et al., 2023). Denitrifying bacteria are involved in nitrate reduction, N loss, and N_2O emissions; their existence is crucial to the soil N cycle even though they only

make up 0.5–5% of the entire microorganism population (Prescott et al., 2014; Canfield et al., 2016).

Denitrification (NO_3^--N→NO_2^--N→NO→N_2O→N_2), a key link in the nitrogen (N) cycle, is an important pathway resulting in the loss of available N in soils (Attard et al., 2011; Li et al., 2021; Lan et al., 2023). Nitrite reductase-mediated reduction of NO_2- to NO is the central step in denitrification because dissolved N becomes gaseous N for the first time (Yin et al., 2014; Yang et al., 2017; Gineyts et al., 2023). Currently, nitrite reductase marker genes (*nirK* and *nirS*) are routinely used, enabling us to revealing abundance and structure of denitrifying microbes in soil samples.

In desert ecosystems, soil microbes are typically severely limited by the availability of water, organic matter, and nutrients. Agricultural practices (such as tillage, fertilization, and irrigation) have a substantial impact on the amount of soil moisture and nutrients available when a native desert is converted to an irrigated area (Su et al., 2010; Wang et al., 2019), which may modify the dynamics of the denitrification community and the potential denitrification rate (PDR) (Attard et al., 2011; Wang et al., 2019). For example, Wu et al. (2021) detected that moisture and fertilizer addition stimulated the activity of *nirK* and *nirS* genes, resulting in an increase in the microbial potential for denitrification in hyperarid Atacama Desert, and similar trends for denitrifier abundance (*nirK* and *nirS*) and PDR were observed in the Omani Desert (Abed et al., 2015). Irrigated cropland soils exhibit an increased abundance and

diversity of denitrifying microbes due to increased soil porosity and liquid water nutrient supply in a Desert-Oasis Ecotone in northwestern China (Chen et al., 2019). Bu et al. (2020) observed that the desertification process resulted in a considerable decrease in soil moisture, available N, and available phosphorus, which in turn led to a decrease in the richness of *nirK* and *nirS*, with a reduction in N loss potential in the Mu Us Desert. In addition, changes in soil texture due to cultivation could also explain changes in denitrifying microbes (Cheng et al., 2018; Wang et al., 2019).

Understanding the community composition of *nirK* and *nirS* genes is an effective way to predict PDR since their abundance and community composition dominate NO3-N reduction as well as N_2O and N_2 emission. However, a quantitative relationship between PDR and community composition of *nirK* and *nirS* in soil along a cultivation chronosequence is unknown. Moreover, the relationship of biological and environmental explanatory variables to the observed changes in PDR following those conversions is still unclear. Here, we aimed to determine the differences in PDR and in the abundance and diversity of denitrifier communities along a cultivation chronosequence made up of uncultivated sandy land (USL, 0 year, never used for agriculture), a young oasis field (YOF, cultivated for 23 years), and an old oasis field (OOF, cultivated for crop production for 54 years). We used gas chromatography, real-time qPCR, and high-throughput pyrosequencing. We hypothesized that agricultural practices following cultivation increase soil denitrification via their positive effects on

the abundance and diversity of the denitrifying community. Our objectives were to (1) quantify the difference in soil PDR following the conversion of native desert to an irrigated field, (2) assess the response to cultivation of the structure of *nirS*- and *nirK*-type denitrifier communities, and (3) identify and rank biological and abiotic drivers that explain the temporal changes in PDR.

2. Materials and methods

2.1 Study site description

The study was directed in Zhangye oasis (100°07′ E, 39°24′ N) in the middle reaches of the Heihe River Basin of Gansu province, China. It has a typical temperate continental climate, with an annual temperature of 7.6°C, annual precipitation of 117 mm, and annual pan evaporation of 2388 mm. According to the World Reference Bade (WRB) classification system, soil is categorized as the Calcic Yermosol; it is often coarse-textured, contains a lot of sand, and has poor water and nutrient retention. (Xiao et al., 2009; Su et al., 2010). The depth of the groundwater level is between 2.5 and 4.5 m due to the fluctuation of the water level of the Heihe River (Wang et al. 2022). Agricultural production depends fully on irrigation, of which about 70% is obtained from groundwater, and the rest from the Heihe River (Wang et al., 2020).

Since the 1950s, sandy lands outside the oasis have progressively been reclaimed for agricultural purposes, resulting in a range of irrigated farmland ages, spanning from 1 year to over 60 years (Zhang et al., 2017). The primary crops cultivated in this region are maize and wheat, with a single annual harvest cycle. Before the year 2000, the

dominant cultivation pattern was wheat-maize intercropping. Since then, approximately 75% of the cropland was switched to a monoculture of seed maize mulched. In recent years, the rate of fertilizer application in maize reached 300-450 kg $N \cdot ha^{-1}$, 90-150 kg $P_2O_5 \cdot ha^{-1}$, and 60-90 kg $K_2O \cdot ha^{-1}$ per year. These fields undergo irrigation 6 to 8 times during each growing season, employing flood irrigation to reach a depth of 600-1200 mm (Su et al., 2017).

In the peripheral desert, some drought-tolerant desert shrub species (*Haloxylon ammodendron*, *Tamarix chinensis*), perennial herb species (*Artemisia desertorum, Kalidium*) and annual sand-fixing plants (*Salsola collina*) have been planted for more than 35 years on sand dunes to protect against sandstorms and to stabilize the dunes (Zhang et al., 2017). The presence of these sand-fixing plants enabled the desert-oasis region to maintain a more stable environment and reduced the incidence of sandstorms by 45% (Luo et al., 2018).

2.2 Experimental design

Two irrigated croplands and one adjacent uncultivated sandy land were used in this study to quantify potential changes in soil denitrification with different cultivation periods. The soil parent material of croplands was the same as that of natural sandy land before agricultural use, and there was no significant difference in soil particle size composition and organic matter content in the initial stage of croplands in the study area (Su et al., 2004).

In this study, five plots (10×30 m) that have been continuously cropped for 54 years ("old oasis field" (OOF)), five plots (18×16 m) that have been cultivated for 23 years ("young oasis field" (YOF)), and five plots (10×30 m) on adjacent sandy land that have never been developed for agricultural use ("uncultivated sandy land" (USL)) were used to conduct the study. The duration of cropland cultivation was determined using records from the Linze Ecological Observational and Experimental Station, Chinese Academy of Sciences, established in 1965. Before the year 2000, all cropland plots underwent wheat (*Triticum aestivum L*) - maize (*Zea mays L*) rotation, with one annual harvest. Since then, maize was grown in monoculture, with plastic film used as mulching. Maize was sown in all cultivated plots on about April 20th and harvested on about September 25th. Conventional tillage was used in YOF and OOF, and the same amounts of fertilizers and irrigation. The fertilization rate was 330 kg N·ha^{-1}, 90 kg P_2O_5·ha^{-1}, and 60 kg K_2O·ha^{-1} each year in the last 20 years. Approximately 90% of irrigation water was sourced from groundwater over the past decade. Cropland plots were irrigated 7 to 9 times depending on soil conditions, with irrigation depth of 100 mm each time.

In October 2020, about one month after maize harvest, 12 topsoil samples (0-20 cm) were collected along the S-shaped transect at each site; samples were composited per plot, stored in ziplock bags and immediately put on ice for transport to the laboratory. In the laboratory, plant residues and litter debris were removed, then soil samples were screened through a 2-mm mesh. Aliquots of fresh samples were stored at -80°C for later

DNA extraction or at 4°C to determine the concentrations of soil inorganic nitrogen and microbial biomass carbon and nitrogen. Remaining samples were air-dried for other physiochemical analyses.

2.3 Physiochemical analysis

Soil pH and soil salinity were determined in 1:2.5 soil:water suspensions. A laser particle analyzer was used to determine the size distribution of soil particles. (Microtrac S3500, Microtrac, USA). Soil ammonium-N (NH_4^+-N, AN) and nitrate-N (NO_3^--N, NN) were extracted with 2M KCL and then determined with an automatic flow-injection analyzer (AA3, Seal Analytical, Bran + Luebbe, Hamburg, Germany). Soil total nitrogen (TN) was determined in a digest of H_2SO_4- $CuSO_4$-K_2SO_4 solution and measured using AA3. Organic matter (OM) was determined with the $K_2Cr_2O_7$-H_2SO_4 oxidation technique, and titration with $FeSO_4 \cdot 7H_2O$.

2.4 Potential denitrification rates

Soil potential denitrification rates (PDR) were calculated using the acetylene (C_2H_2) inhibition approach (Yan et al., 2018). Briefly, 10 g fresh soil was weighed into a 50 ml serum bottle with 20 ml incubation solution containing 0.18 $g \cdot L^{-1}$ glucose, 1.0 $g \cdot L^{-1}$ chloramphenicol, and 0.1 $g \cdot L^{-1}$ KNO_3. All of the bottles were filled with N_2 at least 3 times. C_2H_2 was added to the bottle's headspace in around 10% of the bottle's total volume to prevent N_2O from being reduced to N_2. Bottles were placed on a shaker (100 $rpm \cdot min^{-1}$) and incubated in the dark for 24 h at 25 °C. The N_2O concentrations

were measured by gas chromatography (Agilent 6890 N, Agilent Technologies Inc., USA).

2.5 Microbial analysis

2.5.1 Microbial biomass carbon and nitrogen

The carbon (MBC) and nitrogen (MBN) content of soil microbial biomass were measured using the chloroform fumigation-extraction method (Wu et al., 1990). In a nutshell, 15 g fresh soil was subjected to chloroform for 24 h. Using a vacuum pump to completely remove all of the chloroform, soil samples were extracted using 50 mL of 0.05 mol L^{-1} K_2SO_4. After fumigation and extraction, the total dissolved organic C in the liquid was measured using a total organic C analyzer (Phoenix 8000; Teldyne Tekmar, Mason, OH, USA), and mineral N in the liquid was measured using AA3. The MBC = E_C/K_{EC}, where E_C was the difference between extracted organic C in fumigated soil and non-fumigated soil and K_{EC} of 0.45 was a correction factor; MBN = E_N/K_{EN}, where E_N was the difference between extracted mineral N in fumigated and non-fumigated soil and K_{EN} of 0.54 was a conversion coefficient.

2.5.2 DNA extraction

Deoxyribonucleic acid (DNA) was created from roughly 0.5 g of fresh soil using the FastDNA Spin Kit (MP Biomedical, Carlsbad, CA, USA). Purification and concentration of DNA were determined with 260/280 and 260/230 nm absorbance ratios using a NanoDrop 2000 spectrophotometer (Thermo Fisher Scientific, Waltham,

MA, USA). For subsequent testing, qualified DNA was kept in a freezer at -20 °C.

2.5.3 Quantitative PCR

Numerous studies have employed the genes *nirK* and *nirS* as functional gene markers to determine the abundance of nitrifying and denitrifying bacteria (Gao et al., 2020). The qPCR reactions were carried out in ABI PRISM 7300 Sequence Detection System (Applied Biosystems, USA). The 20.0 μL reaction mixture contained 10.0 μL of 2X Taq Plus Master Mix (ChamQ SYBR Color qPCR Master Mix (2X), Nanjing, China), 0.8 μL of each forward and reverse primers (5 μM), 1.0 μL of template DNA, and 7.4 μL of ddH_2O. The standard curve of *nirK* and *nirS* was obtained using a 10-fold dilution of functional gene plasmids DNA, with R^2 ranging from 0.993 to 0.997. The qPCR reaction of the *nirK* and *nirS* gene was 5 min at 95°C, and the subsequent thermal profile of the four genes (Table 1). The gene copy numbers for *nirK* and *nirS* were calculated based on the relationship between the standard concentration and the converting cycle threshold (Ct) value using external standard methods. Based on Eff = $[10(^{-1/slope})-1] \times 100\%$, the amplification efficiencies of *nirK* and *nirS* were 87.9 and 87.4%, respectively.

2.5.4 PCR amplification

The diversity and gene-community composition of *nirK* and *nirS* were determined using the polymerase chain reaction (PCR). Sequencing was done using the primers LWC-*nirK* F/R (*nirK*) and *nirS* 4F/6R (*nirS*) (Table 1). Independent PCR amplifications

were conducted in triplicate on ABI GeneAmp® 9700 (ABI, USA). The PCR reaction was provided in 20.0 μL including 4.0 μL of 5×FastPfu Buffer, 2.0 μL of 2.5 mM dNTPs, 0.8 μL of each forward and reverse primers (5 μM), 0.4 μL of FastPfu Polymerase, 0.2 μL BSA, 10.0 ng of DNA template, and 1.8 μL ddH_2O. All genes underwent 37 cycles of denaturation at 95 °C for 30 seconds, annealing at 60 °C for 30 seconds, extension at 72 °C for 45 seconds, and final extension at 72 °C for 10 minutes. PCR products were purified with AxyPrep DNA Gel Extraction Kit (Axygen Biosciences, Union City, CA, USA), detected with 2% agarose gel electrophoresis, and quantified with Quantus™ Fluorometer (Promega, USA). NEXTFLEX Rapid DNA-SEQ Kit was used for DNA library construction. Amplicon sequencing was performed on the Illumina MiSeq PE300/NovaSeq PE250 platform (Majorbio Company, Shanghai, China).

2.5.5 Bioinformatics analysis

The PE reads by Miseq sequencing were spliced, controlled, and filtered to obtain valid sequences using Quantitative Insights Into Microbial Ecology (QIIME) (https://docs.qiime2.org, version:17.0) (Bolyen et al., 2019). Primers, low-quality sequences (quality score <20; homologs longer >10 bp; length < 150 bp; with one or more ambiguous bases), duplicated sequences, and single sequences without repetition were removed using fastp (https://github.com/OpenGene/fastp, version 0.20.0) (Chen et al., 2018; Chen et al., 2021). The remaining reads were spliced based on the overlap

relation between PE reads using FLASH (http://www.cbcb.umd.edu/software/flash，version 1.2.7) (Magoč and Salzberg, 2011). Representative sequences of operational taxonomic units (OTUs) sequence cluster (excluding chimera) with a sequence identity threshold of 97% were performed with UPARSE program (http://drive5.com/uparse/,version 7.0.1090) (Edgar, 2013). Representative sequences of OTUs were generated by selecting the most abundant sequences, and OTUs with abundance < 0.001% were discarded (Bokulich et al., 2013). A total of 1298 and 499 OTUs were obtained for *nirK* and *nirS*, respectively. Ribosomal Database Project (RDP) naïve Bayesian classifier (http://sourceforge.net/projects/rdp-classifier/, version 2.11) was used to classify the *nirK* and *nirS* genes OTUs to taxonomic groups at 70% confidence threshold base with GeneBank database (Release7.3 http://fungene.cme.msu.edu/) (Fish et al., 2013). Community alpha diversity were calculated using the Chao1 (Chao, 2003) and Shannon indices (Chao and Shen, 2003); community beta diversity was examined with PCoA (Chen et al., 2021).

2.6 Statistical analysis

All data were tested for normality in SPSS 21.0 (Chicago, IL, USA) before statistical analysis. One-way analysis of variance (ANOVA) and Least Significance Difference (LSD) were applied to assess differences in soil properties, absolute and relative abundances, OTUs number, coverage, and alpha diversity indices (Chao1 index and Shannon index) among USL, YOF, and OOF. The Alpha diversity index of *nirK*

and *nirS* genes consisted of OTUs at OTU level. The community composition of *nirK* and *nirS* genes consisted of OTUs at genus level. Kruskal-Wallis H test was adopted to examine species abundance differences at phylum level among sampling sites. Principal Component Analysis (PCoA) and ANOSIM test were performed to assess variations in the community composition of *nirK* and *nirS* genes among sampling sites (USL, YOF and OOF) based on Bray Curtis dissimilarities using vegan package in R Studio 3.5.2 software (http://cran.r-project.org/).

Partial least squares path modeling (PLS-PM) was conducted to assess the connections among soil properties, microbial communities, and PDR. PLS-PM is the extension of a multiple linear regression model, which is often used to investigate complex multivariate relationships between predictor and response variables (Sanchez, 2013). The R package 'plspm' was used to construct the model. The acceptable range of goodness of fit (GoF) and average variance extracted (AVE) were $0.40 < GoF < 1.0$, and $AVE > 0.5$, respectively (Vanalle et al. 2017). In the model, eight latent variables were used, namely, (1) soil physical properties, (2) soil chemical properties, (3) microbial biomass, (4) richness and (5) abundance of *nirK* and *nirS* genes, (6) alpha-diversity and (7) beta-diversity of *nirK* and *nirS* genes, and (8) PDR. SMC, sand content, and BD represented soil physical properties; pH, salinity, AN, NN, and OM represented soil chemical properties, MBC and MBN represented microbial biomass; the number of OTUs, and the copy numbers of *nirK* and *nirS* genes represented richness and

abundance, respectively; the Shannon and Chao1 indices, and the first axes from a PCoA analysis within the OTU community matrix (PC1) of *nirK* and *nirS* genes represented the alpha- and beta-diversity, respectively.

3. Results

3.1 Soil properties and PDR

Soil BD and particle size distribution differed significantly across cultivation types (Fig. 1b and c). Sand content at USL was > 90%, while that at YOF and OOF was lower than at USL ($P < 0.05$); soils were correspondingly classified as sandy at USL, sandy loam at YOF, and loamy at OOF, based on the United States Department of Agriculture (USDA) soil classification. Soil pH was greater at OOF than at USL ($P < 0.05$), but the soil salinity did not alter over the course of cultivation (Fig. 1d and e). Sites exhibited a significant increase in soil moisture (Fig. 1a) and soil nutrients (Fig. 1f-h and 1k-l), but a significant reduction in soil C/N ratio (Fig. 1j) with cultivation time ($P < 0.05$). Contents of AN, NN, and TN at OOF were 6.9, 38.5, and 6.4 times greater than at USL. OM at USL, YOF, and OOF was 4.88, 16.03, and 21.5 $g \cdot kg^{-1}$, respectively. As cultivation time increased, the content of MBC and MBN increased from 15.92 $g \cdot kg^{-1}$ at USL to 129.95 $g \cdot kg^{-1}$ at OOF for MBC, and from 62.12 $g \cdot kg^{-1}$ at USL to 316.8 $g \cdot kg^{-1}$ at OOF for MBN.

PDR increased significantly with the increase in cultivation time ($P = 0.001$) (Fig. 2). PDR at USL, YOF, and OOF was 10.08 ± 2.88, 23.68 ± 3.62 and 52.8 ± 6.78 $\mu g \cdot g^{-1} \cdot d^{-1}$, respectively.

3.2. Abundance of denitrifying microbes

Absolute abundances of *nirK* and *nirS* genes were significantly affected by the cultivation period and significantly increased from USL to OOF ($P = 0.001$) (Fig. 3). The average abundance of *nirK* genes copies per gram of dry soil ranged from 1.03×10^6 to 6.33×10^7(Fig. 3a), whereas that of *nirS* genes copies ranged from 4.25×10^3 to 5.40×10^6 (Fig. 3b); this indicated that copy numbers of *nirK* dominated in the desert oasis soil. In addition, ratios of *nirK* to *nirS* in YOF and OOF were generally one order of magnitude greater than those in USL ($P = 0.001$) (Fig. 3c).

3.3. Community and diversity of denitrifying microbes

3.3.1 Community composition

A total of 27 *nirK* gene genera was detected in all soil samples. We found 10, 23, and 25 *nirK* gene genera in USL, YOF, and OOF soils, respectively. Ten *nirK* gene genera were common across the three sites. The number of *nirK* gene genera in YOF and OOF soil was significantly greater than that in USL. The predominant genera with the *nirK* gene were significantly different among the three sampling sites. At USL, nearly 80% of genera species run to completion in unclassified_k__norank_d__Bacteria, followed by unclassified_d__Unclassified (15.1%). However, in YOF and OOF, unclassified_k__norank_d__Bacteria, Sinorhizobium, Ensifer, unclassified_f__Bradyrhizobiaceae, and unclassified_o__Rhizobiales jointly dominate *nirK* gene communities (Fig. 4a).

We detected 15 *nirS* functional gene genera in the three sites. We found 3,10 and 14 *nirS* gene genera in USL, YOF, and OOF soils, respectively. Three *nirS* gene genera were common across the three sites. unclassified_p__Proteobacteria (45.3%), unclassified_k__norank_d__Bacteria (46.4%) and unclassified_c__Betaproteobacteria (8.3%) dominated the *nirS* gene community in USL. The predominant *nirS* species were largely consistent in YOF and OOF; however, differences in relative abundances were observed (Fig. 4b). In YOF and OOF, the dominant species were unclassified_p_Proteobacteria, unclassified_k__norank_d__Bacteria, and norank_p__environmental_samples, accounting for 65.4, 20.0, and 9.8% of the relative abundance in YOF, and 49.7, 24.1, and 19.8% in OOF, respectively.

3.3.2 Community richness and diversity

The full dataset yielded a total of 244929 *nirK* gene sequences and 297416 *nirS* gene sequences, and a total of 1298 OTUs for *nirK* gene and 499 OTUs for *nirS* gene were discovered. All samples had *nirK* and *nirS* gene coverage levels that were above 99% (Fig. 5 a and e), indicating that the number of *nirK* and *nirS* genes sequences obtained represented *nirK* and *nirS* genes communities well.

Cultivation significantly affected the number of OTUs; OTUs number of *nirK* and *nirS* genes increased significantly with the increase in cultivation time (Fig. 5 b and f). The conversion from native desert soils to irrigated croplands significantly increased richness and diversity of *nirK* and *nirS* gene communities. The Chao1 index

of *nirK* and *nirS* genes and the Shannon index of *nirK* genes differed significantly among USL, YOF, and OOF (Fig. 5 c, d and g). The Shannon index of *nirS* gene in cultivated fields (YOF and OOF) was significantly higher than that in uncultivated sandy land (Fig. 5h).

The PCoA of community β-diversity clearly grouped the *nirK* and *nirS* genes communities according to the three sampling sites (Fig. 7 a and b). The first two axes (PC1 and PC2) explained 99.68 and 91.4%, respectively, of the total variance for *nirK* and *nirS* genes communities. In addition, the ANOSIM test revealed a significant difference among USL, YOF and OOF (P =0.001) along coordinate 1 in the compositions of *nirK* and *nirS* communities at the phylum level (Fig. 6).

3.3.3 Community differences

At the phylum level, in USL, two groups of *nirK* genes community and one group of *nirS* geness community were significantly enriched as indicated by the Kruskal-Wallis H test, these were unclassified_k__norank_d__Bacteria, unclassified_d__Unclassified (Fig. 7a) and unclassified_k__norank_d__Bacteria (Fig. 7b). Proteobacteria phyla were significantly enriched in YOF of *nirK* and *nirS* genes community (Fig. 7 a,b). In OOF, 2 groups of *nirK* genes community and 2 groups of *nirS* genes community were significantly enriched, namely Proteobacteria, environmental_samples_k__norank_d__Bacteria (Fig. 7a), Proteobacteria and environmental_samples (Fig. 7b). At the phylum level, the relative abundance of

Euryarchaeota in *nirK* genes community (Fig. 7a) and unclassified_d__Unclassified in *nirS* genes community (Fig. 7b) showed no significant difference among USL, YOF and OOF as summarized by the Kruskal-Wallis H test.

3.4 Relationships among PDR, soil properties, and denitrifiers

The PLS-PM results (GOF = 0.854) showed that soil physical properties, soil chemical properties, and microbial biomass affect PDR directly, and also indirectly, by changing the abundance and community structure of denitrifiers (Fig. 8b). Soil physical properties had a negative effect on PDR, with a direct effect of -0.6004 and an indirect effect of -0.018 (Fig. 8a and b); within that, sand content had the strongest effect on PDR (Table 2).

The direct positive path coefficient of soil chemical properties effect on PDR was 0.987, while the indirect path coefficient was -0.847; the resulting total effect of soil chemical properties on PDR did not reach the significant level ($P > 0.05$). Soil chemical properties of AN, NN, and C/N had the strongest positive effect on PDR (Table 2).

Microbial biomass had direct negative and indirect positive effects on PDR, with path coefficients of -0.517 and 0.773, respectively (Fig. 8b). Beta-diversity had significant negative effects on PDR, while richness and abundance had significant positive effects on PDR, with path coefficients of -0.901, 0.864 and 0.604, respectively.

4. Discussion

4.1 Responses of soil properties to cultivation

In arid regions, uncultivated sandy soils typically display a loose structure and possess low levels of water and nutrients due to prolonged wind erosion (Chen et al., 2019). Following the transformation of uncultivated sandy soil into cropland, the processes of tillage, irrigation, and fertilization exert significant effects on soil formation. These practices enhance soil structure and elevate soil moisture and nutrient levels (Su et al., 2010; Su et al., 2017; Zhang et al., 2017). In this study, we observed that silt and clay concentrations increased with the duration of cultivation, while bulk density decreased (Fig. 1b and c). The rise in silt and clay content primarily resulted from the continuous inflow of sediment carried by irrigation water from the Heihe River. Research indicates that the irrigation of Heihe River water, which contains silt, can transport over 2500 kg • hm^{-2} • y^{-1} of particles into the cropland (Su et al., 2017). The introduction of clay had a substantial positive impact on the formation of soil aggregates and led to a reduction in bulk density in these arid soils (Zhang et al., 2018).

Soil SMC, AN, NN, TN, OM, MBC and MBN exhibited substantial increases with prolonged cultivation time (Fig.1a, f-l). The favorable trend in soil moisture and nutrient enhancement can be attributed to agricultural practices. Agricultural manure and irrigation increased the input of organic cementing materials, and crop residues increased the input of biomass and nutrients to the soil, promoting soil evolution

(Saviozzi et al. 2001). In addition, fertilization and irrigation increased crop yield, which in turn increased the input of organic carbon and nitrogen through litter and roots, resulting in a positive transformation of soil fertility (Lozano et al. 2014). Cultivation also resulted in a significant decrease in soil pH, which may be related to the accumulation of organic acids secreted by crop roots and the leaching of alkaline ions due to high volumes of irrigation (Li et al. 2015; Chen et al. 2019).

4.2 Responses of denitrifiers to cultivation

There was mounting evidence that the abundance and diversity of denitrifiers are sensitive to agricultural practices (Li et al., 2014; Yang et al., 2017; Wang et al.,2019) especially in desert soils in arid climates (Lozano et al. 2014; Wu et al.,2021). The *nirK* and *nirS* genes can reduce NO_3^- to NO through denitrification and are commonly-used metabolic markers (Barta et al., 2010). In this study, the abundance of *nirK* and *nirS* genes significantly increased with the cultivation period (Fig. 3a and b). This might be the result of prolonged cultivation increasing moisture and substrate in the plough layer, where a deficiency in oxygen was favorable for denitrifier development (Yin et al., 2014; Wu et al.,2021). The higher SMC and NO_3^-N content in YOF and OOF in this study also supported such an effect (Fig. 1a and g). Herold et al. (2018) and Wang et al.(2019) observed that denitrifying bacteria prefer to grow in a weakly alkaline soil environment; thus, the reduction in pH following cultivation (Fig. 1d) may also promote the higher abundance of denitrifiers in YOF and OOF.

Previous studies have shown that the *nirK* gene often exhibited higher abundance than the *nirS* gene in different tillage, irrigation and fertilization systems (Tang et al., 2020); this is consistent with our results, but contrary to the result of Wang et al. (2019), Xiao et at. (2021) and Wang et al. (2022). *nirK* gene abundance was at least an order of magnitude higher than *nirS* gene abundance in all three treatments, and it was 23.5 orders of magnitude higher in USL. However, despite *nirK* gene abundance increasing with continuous cultivation, *nirS* gene increase rate was much higher than NirK gene increase rate (Fig. 3c). Similar results have been reported in other studies; *nirS*-type denitrifiers appear to be more sensitive to moisture and available nitrogen addition in hyperarid desert soils (Wu et al., 2021), paddy soils (Xiao et al., 2021) and dryland soils (Wang et al., 2022) than *nirK*-type denitrifiers. The differences between *nirK* and *nirS* genes are likely due to distinctive niche preferences of the functional genes, and *nirK* genes may preferentially participate in denitrification in nitrogen-deficient soil, while *nirS* genes may be more sensitive to available water and nutrient additions (Wu et al., 2021). Thus, the higher rate of increase of *nirS* than of *nirK* may be attributed to increased soil moisture and nutrients following cultivation.

Sequencing results showed that *Sinorhizobium*, *Bradyrhizobiaceae*, *Ensifer*, *Rhizobiales*, *Rhodanobacter* and *Proteobacteria* are the dominant genera in proteobacterial phyla in YOF and OOF (Fig, 4). Bacterial phyla decreased and proteobacterial phyla increased both in *nirK* and *nirS* community following cultivation

(Fig, 4 and 7). The OTU number and α-diversity index (Chao1 and Shannon) in *nirK* and *nirS* communities increased with the increase in the cultivation period (Fig, 5). The PCoA clearly grouped *nirK* and *nirS* gene communities (Fig, 6). The Kruskal-Wallis H test indicated significant species differences among USL, YOF, and OOF (Fig, 7). These results support our hypothesis that cultivation can shape a microbial community structure, alter denitrifier community and diversity composition, and alter soil ecosystem functions. In this study, *proteobacterial* phyla were the common dominant phyla of *nirK* and *nirS* community in irrigated cropland soil (YOF and OOF), which was consistent with results for saline and alkaline soils (Yang et al., 2018), paddy soils (Xiao et al., 2021), and dryland soils (Wang et al., 2022). Wei et al. (2015) and Shapleigh (2013) also showed that most denitrifying bacteria belonged to *proteobacterial* phyla, and an increase in their abundance was conducive to denitrification. Bacterial phyla play an important role in an uncultivated desert soil (USL), confirming the results of Wu et al. (2021), who also found that bacteria were a dominant phylum in a denitrifier community in arid and barren desert soil. The differences between an uncultivated desert soil and an irrigated cropland soil in *nirK* and *nirS* community are likely due to a different composition of dominant strains in *nirK* and *nirS* communities, with different strains of denitrifiers responding to different stresses in their environment (Attard et al., 2010).

4.3 Relative importance of edaphic factors and denitrifiers for explaining variation in PDR

The PLS-PM revealed a clear difference between abiotic (edaphic) and biological factors in explaining the variation in PDR (Fig.8b). Specifically, the abundance and diversity of denitrifiers exert a direct influence on soil PDR, whereas soil properties indirectly modulate PDR by regulating microbial activity (Fig.8a). Soil physical properties, such as soil bulk density and sand content, were notably reduced through cultivation, leading to increased soil capillary pores (Wang et al., 2019). Such a favourable trend in soil texture is conducive to water storage and provides a local anaerobic environment for denitrification (Enwall et al., 2005; Lozano et al., 2014).

Soil chemical properties exhibited a direct positive impact on denitrifier abundance and diversity, with the highest loading coefficients observed for pH, NO_3^--N, organic matter, and microbial biomass carbon and nitrogen (Table 2). Notably, a strong negative association between soil pH and PDR was evident, with a standardized loading coefficient of -0.911 (Table 2). Our study recorded pH levels between 7.8 and 8.9 (Fig. 1), falling outside the optimal pH range for denitrification, which typically ranges from 6.5 to 7.5 (Li et al., 2021). According to Wang et al. (2019), higher pH inhibits the growth of denitrifying bacteria to some extent and reduces the amount of organic carbon and mineral nitrogen available to denitrifying microorganisms. As a reactant of denitrification, soil NO_3^--N has a load coefficient with PDR of up to 0.923

(Table. 2). Previous research has demonstrated that PDR increases with greater NO_3^--Nlevels (Chen et al., 2019; Wang et al., 2019) due to the heightened activity and abundance of denitrifying bacteria in the presence of elevated NO_3^--Nlevels (Yang et al., 2014; Xiao et al., 2021). Additionally, the NO_3^--N content increased along with the enzymatic activity of denitrification, including nitrate reductase activity (Ye et al., 2021) and nitrite reductase activity (Xu et al., 2023). It is necessary for organic carbon to be available as a substitute electron donor and for NO_3^--N to be available as an electron acceptor for the facultative process of denitrification (Attard et al., 2010). In agricultural ecosystems, the accumulation of organic matter resulting from agricultural practices not only supplies electrons for denitrification but also serves as an organic substrate supporting the growth and activities of denitrifying microorganisms (Su et al., 2010; Wang et al., 2019). Furthermore, the consumption of oxygen during the decomposition of organic waste fosters the development of an anaerobic environment, expediting denitrification (Li et al., 2021). It is worth noting that microbial biomass exhibited a negative effect on denitrifier abundance and richness (Fig. 7a), potentially due to the limitations of soil microbial C and N pools in accurately reflecting the availability of carbon and nitrogen (Chen et al., 2019).

The positive influence of denitrifier abundance on PDR aligns with findings in soils subjected to both conventional tillage and no-tillage practices (Baudoin et al., 2009), conversions from grassland to cropping systems (Attard et al., 2010), and long-

term agricultural fertilization systems (Wang et al., 2022). Additionally, during the ecological restoration of abandoned farmland, Wang et al. (2019) observed that a higher abundance of nirK and nirS genes correlated with increased PDR. Mineral and organic fertilizers can raise the *nirK* and *nirS* gene abundance, which could boost the capacity for potential denitrification activity (Tang et al., 2020). Similarly, Attard et al. (2010) observed an increase in PDR after cultivation, and this was largely coupled with changes in the abundance of *nirK* and *nirS* genes. In this study, soil structure and fertility exhibited a favourable trend (Fig.1) with an increase in cultivation period, stimulating the growth of denitrifying microorganisms (Fig.3 and 4) which had a significant positive effect on PDR (Fig.2). These observations underscore the pivotal role of *nirK* and *nirS* gene abundance as an integrative ecological variable for predicting and elucidating the dynamics of PDR during the process of oasis development.

Under certain conditions, different species or strains of denitrifiers can have different physiological or metabolic features and can generate different levels of denitrification (Salles et al., 2009). Consequently, the relationship between the community diversity of denitrifiers and PDR remains uncertain, with conflicting findings reported in the literature (Graham et al., 2016; Wang et al., 2019). It is improbable that community diversity alone can explain concurrent PDR levels, potentially due to the dominant influence of real-time edaphic variables on these rates. Random fluctuations in edaphic variables can lead to substantial variations in PDR

while having minimal impact on community diversity (Wang et al., 2019). Attard et al. (2010) also found that it edaphic conditions rather than denitrifying communities drove the variation in PDR after changes in land use. Additionally, microbial communities might be more important in high PDR than low PDR. (Hallin, et al., 2009). In this study, PLS-PM showed that α-diversity had no significant effects on PDR, while β-diversity had a significant negative effect on PDR (Fig.8a). Similarly, Sainur et al. (2016) observed that α-diversity had no significant relationship to PDR in arid pasture soil ecosystems. Wang et al. (2019) detected a negative relationship between β-diversity and PDR in plant-restored soils.

Conclusions

Our findings showed that cultivation enhanced soil nutrient and organic C pools, decreased bulk density, and increased soil clay content in a desert soil. This favorable trend in soil structure and fertility increased the abundance and diversity of denitrifying communities, leading to higher soil PDR in irrigated oasis cropland. Therefore, the changes in soil properties caused by tillage increase the potential gaseous N loss to some extent during the process of desert soil oasization. The *nirK*-type denitrifying community appeared to be the main drivers of denitrification, but *nirS*-type denitrifying community may be more sensitive to cultivation. The composition of the denitrifier community changed as a result of continuous cultivation, namely with a negative influence on bacterial phyla and a favorable impact on proteobacterial phyla. Moreover,

our results also indicate that the variation in PDR was mainly explained by the abundance and β-diversity of denitrifiers. Our results increased the understanding of the evolution of denitrifying communities and potential N losses, particularly during an extensive conversion of natural desert into agricultural land of northwestern China.

Acknowledgements

Funding information: This research was jointly supported by the Second Tibetan Plateau Scientific Expedition and Research (STEP) program (No. 2019QZKK0303) and the National Natural Science Foundation of China (No. 32071635). We are grateful to Dr. Xiangyan Feng for providing the photos.

Data Availability :

The data that support the findings of this study are available from the corresponding author upon reasonable request.

References

Abed R M M, De Beer D, Stief P. Functional-Structural Analysis of Nitrogen-Cycle Bacteria in a Hypersaline Mat from the Omani Desert. Geomicrobiology Journal, 2015, 32(2):119-129.

Attard, E, Recous, S, Chabbi, A, et.al. Soil environmental conditions rather than denitrifier abundance and diversity drive potential denitrification after changes in land uses. Global Change Biology. 2011, 17(5): 1975-1989.

Barta, J, Melichova, T, Vanek, D, et al. Effect of pH and dissolved organic matter on the abundance of *nirK* and *nirS* denitrifiers in spruce forest soil. Biogeochemistry. 2010.101, 123-132.

Baudoin, E, Philippot, L, Che`neby, D, et al. Direct seeding mulch-based cropping increases both the activity and the abundance of denitrifier communities in a tropical soil. Soil Biology and Biochemistry. 2009, 41, 1703-1709.

Bokulich, N A, Subramanian, S, Faith, J J, et al. Quality filtering vastly improves diversity estimates from Illumina amplicon sequencing. Nature Methods. 2013,10, 57-60.

Bolyen, E, Rideout, J M, Matthew, R, et al. Reproducible, interactive, scalable and extensible microbiome data science using QIIME 2. Nature Biotechnology. 2019, 37, 848-857.

Bu L, Peng Z, Tian J, et al. Distinct abundance patterns of nitrogen functional microbes in desert soil profiles regulate soil nitrogen storage potential along a desertification development gradient. Catena, 2020, 194:104716.

Canfield, D E, Glazer, A N, Falkowski, P G. The evolution and future of Earth's nitrogen cycle. Science, 2016, 330 (6001),192-196.

Chao, A, Shen, T J, Nonparametric estimation of Shannon's index of diversity when there are unseen species in sample. Environmental and Ecological Statistics. 2003, 10, 429-443.

Chen, L F, He, Z B, Zhao, W Z, et al. Soil structure and nutrient supply drive changes in soil microbial communities during conversion of virgin desert soil to irrigated cropland. European Journal of Soil Science. 2019, 71 (4): 768-781

Chen, S, Zhou, Y, Chen, Y, et al. fastp: an ultra-fast all-in-one FASTQ preprocessor. Bioinformatics. 2018, 34(17):884-890.

Chen, Z J, Jin, Y Y, Yao, X, et al. Gene analysis reveals that leaf litter from Epichlo endophyte-infected perennial ryegrass alters diversity and abundance of soil microbes involved in nitrification and denitrification - ScienceDirect. Soil Biology and Biochemistry. 2021,154,108123

Chen, Z, Ma, J, Liu, Y, et al. Differential responses of soil *nirS*-and *nirK*-type denitrifying microbial communities to long-term application of biogas slurry in a paddy soil. Applied Soil Ecology, 2023, 182: 104711.

Edgar, R C, UPARSE: highly accurate OTU sequences from microbial amplicon reads. Nature Methods. 2013;10(10):996-998.

Enwall, K, Philippot, L, Hallin, S, Activity and composition of the denitrifying bacteria community respond differently to long-term fertilization. Applied and Environmental Microbiology. 2005, 71: 8335-8343

Fish, J A, Chai, B, Wang, Q, et al. FunGene: the functional gene pipeline and repository. Front. Microbiol. 2013, 4, 291.

Gao, S, Zhou, G, Liao, Y, et al. Contributions of ammonia-oxidising bacteria and archaea to nitrification under long-term application of green manure in alkaline paddy soil. Geoderma. 2020, 374:114419.

Gineyts, R, Niboyet, A. Nitrification, denitrification, and related functional genes under

elevated CO_2: A meta-analysis in terrestrial ecosystems. Global Change Biology, 2023, 29(7): 1839-1853

Graham, E B, Knelman, J E, Schindlbacher, A, et al. Microbes as engines of ecosystem function: When does community structure enhance predictions of ecosystem processes? Frontiers in Microbiology. 2016, 7:214.

Hallin, S, Jones, C M, Schloter, M, et al. Relationship between N-cycling communities and ecosystem functioning in a 50-year-old fertilization experiment. The ISME Journal. 2009, 3(5):597-605.

Herold, M B, Giles, M E, Alexander, C J, et al. Variable response of *nirK* and *nirS* containing denitrifier communities to long-term pH manipulation and cultivation. Fems Microbiology Letters. 2018, 80 (6),365-374.

Lan, T, Li, M, He, X, et al. Effects of exogenous carbon and nitrification inhibitors on denitrification rate, product stoichiometry and *nirS/nirK*-type denitrifiers in a calcareous soil: evidence from 15 N anaerobic microcosm assays. Journal of Soils and Sediments, 2023: 1-16.

Li, C H, Tang, L S, Jia, Z J, et al. Profile changes in the soil microbial community when desert becomes oasis. PLoS One. 2015, 10 (10): e0139626.

Li, Y, Chen, Z, Lou, H, et al. Denitrification controls in urban riparian soils: implications for reducing urban nonpoint source N pollution. Environmental Science and Pollution Research. 2014, 21(17): 10174-10185.

Li, Z, Tang Z, Song, Z P., et al. Variations and controlling factors of soil denitrification rate. Global Change Biology. 2021, 9 (28):2133-2145.

Li, Z, Tiang, Z, Song, Z P, et al. Variations and controlling factors of soil denitrification rate. Global Change Biology. 2021, 28(6): 2133-3145.

Lozano, Y M, Hortal, S, Armas, C, et al. Interactions among soil, plants, and microorganisms drive secondary succession in a dry environment. Soil Biology and Biochemistry. 2014, 78: 298-306.

Luo, W, Zhao, W, Zhuang, Y. Sand-burial and wind erosion promote oriented-growth and patchy distribution of a clonal shrub in dune ecosystems. Catena. 2018, 167:212-220.

Magoč, T, Salzberg, S L, FLASH: fast length adjustment of short reads to improve genome assemblies. Bioinformatics. 2011,27(21):2957-2963.

Prescott, C E, Levy B, et al. Microbial functional genes involved in nitrogen fixation, nitrification and denitrification in forest ecosystems. Soil Biology & Biochemistry, 2014,75:11-25.

Sainur, S M, Bakken, L R, Shahid, N. High-resolution denitrification kinetics in pasture soils link N_2O emissions to pH, and denitrification to C mineralization. PLoS One. 2016,11(3): e0151713.

Salles, J F, Poly, F, Schmid, B, et al. Community niche predicts the functioning of denitrifying bacterial assemblages. Ecology. 2009, 90: 3324-3332.

Sanchez, G, PLS Path Modeling with R. Trowchez Editions, Berkeley. 2013

Saviozzi, A, Levi-Minzi, R, Cardelli, R, et al. A comparison of soil quality in adjacent cultivated, forest and native grassland soils. Plant Soil. 2001, 233, 251-259.

Su, Y Z, Yang, R, Liu, T N, et al. Changes in soil properties and accumulation of soil carbon after cultivation of desert sandy land in a marginal oasis in Hexi corridor region, Northwest China. Scientia Agricultura Sinica. 2017,50(9):1646-1654.

Su, Y Z, Yang, R, Liu, W J, et al. Evolution of soil structure and fertility after conversion of native sandy desert soil to irrigated cropland in arid region, China. Soil Science. 2010, 175 (5): 246-54.

Su, Y, Z, Zhao, H L, Zhang, T H, et al. Soil properties following cultivation and non-grazing of a semi-arid sandy grassland in northern China. Soil & Tillage Research. 2004, 75(1):27-36.

Szukics, U, Hackl, E, Zechmeister, B S, et al. Contrasting response of two forest soils to N input: rapidly altered NO and N_2O emissions and *nirK* abundance. Biology and Fertility of Soils. 2009, 45, 855-863.

Tang, H M, Li, C, Cheng, K K. Effects of short-term soil tillage management on activity and community structure of denitrifiers under double-cropping rice field. Journal of Microbiology and Biotechnology. 2020,30:1688-1696.

Vanalle, R M, Ganga, G M, Godinho, M, et al. Green supply chain management: an investigation of pressures, practices, and performance within the Brazilian

automotive supply chain. Journal of Cleaner Production. 2017,151: 250-259.

Wang, H L, Shu, D T, Liu, D, et al. Passive and active ecological restoration strategies for abandoned farmland leads to shifts in potential soil N loss by denitrification and soil denitrifying microbes. Land Degradation and Development. 2019, 31:1086-1098.

Wang, L S, He, Z B, Li, J. Assessing the land use type and environment factors affecting groundwater N in an arid oasis in northwestern China. Environmental Science and Pollution Research. 2020, 27(32): 40061-40074.

Wang, X Y, Li, Y J, He, P, et al. Response of soil denitrification potential and community composition of denitrifying bacterial to different rates of straw return in north-central China. Applied Soil Ecology. 2022, 170, 104321.

Wu, D, Senbayram, M, Moradi, G, et al. Microbial potential for denitrification in the hyperarid Atacama Desert soils. Soil Biology and Biochemistry. 2021,157,108248

Wu, J, Joergensen, R G, Pommerening, B, et al. Measurement of soil microbial biomass C by fumigation–extraction–an automated procedure. Soil Biology and Biochemistry. 1990, 22, 1167-1169.

Xiao, G L, Yin, K L, Feng, M L, et al. Changes in soil organic carbon, nutrients and aggregation after conversion of native desert soil into irrigated arable land. Soil & Tillage Research. 2009, 104(2):263-269.

Xiao, X, Xie, G X, Yang, Z H, et al. Variation in abundance, diversity, and composition

of *nirK* and *nirS* containing denitrifying bacterial communities in a red paddy soil as affected by combined organic-chemical fertilization. Applied Soil Ecology. 2021,166,104001.

Xu, C M, Xiao, D S, Chen S, et al. Changes in the activities of key enzymes and the abundance of functional genes involved in nitrogen transformation in rice rhizosphere soil under different aerated conditions. Journal of Integrative Agriculture, 2023, 22(3):923-934.

Xue, J G, Dong, W L, Jia Q S, et al. Oasification: An unable evasive process in fighting against desertification for the sustainable development of arid and semiarid regions of China. Catena, 2019, 179, 197-209

Yang, Y D, Hu, Y G, Wang, Z M, et al. Variations of the *nirS*-, *nirK*-, and *nosZ*-denitrifying bacterial communities in a northern Chinese soil as affected by different long-term irrigation regimes. Environmental Science and Pollution Research. 2018, 25:14057-14067.

Yang, Y, Zhao, J, Jiang, Y, et al. Response of bacteria harboring *nirS* and *nirK* genes to different N fertilization rates in an alkaline northern Chinese soil. European Journal of Soil Biology. 2017, 82:1-9.

Ye, M, Yin, C, Fan, X, et al. Procyanidin inhibited N_2O emissions from paddy soils by affecting nitrate reductase activity and *nirS*- and *nirK*-denitrifier populations. Biology and Fertility of Soils. 2021, 57, 935-947 2021.

Yin, C, Fan, F L, Song, A I, et al. Different denitrification potential of aquic brown soil in Northeast China under inorganic and organic fertilization accompanied by distinct changes of *nirS*- and *nirK*-denitrifying bacterial community-ScienceDirect. European Journal of Soil Biology. 2014, 65:47-56.

Zhang, Y Y, Zhao, W Z, Fu, L. Soil macropore characteristics following conversion of native desert soils to irrigated croplands in a desert-oasis ecotone, Northwest China. Soil & Tillage Research. 2017, 168 (2): 176-186.

Zhang, Y Y, Zhao, W Z, He, J H, et al. Soil susceptibility to macropore flow across a desert-oasis ecotone of the Hexi corridor, Northwest China. Water Resources Research. 2018, 54(2):1281-1294.

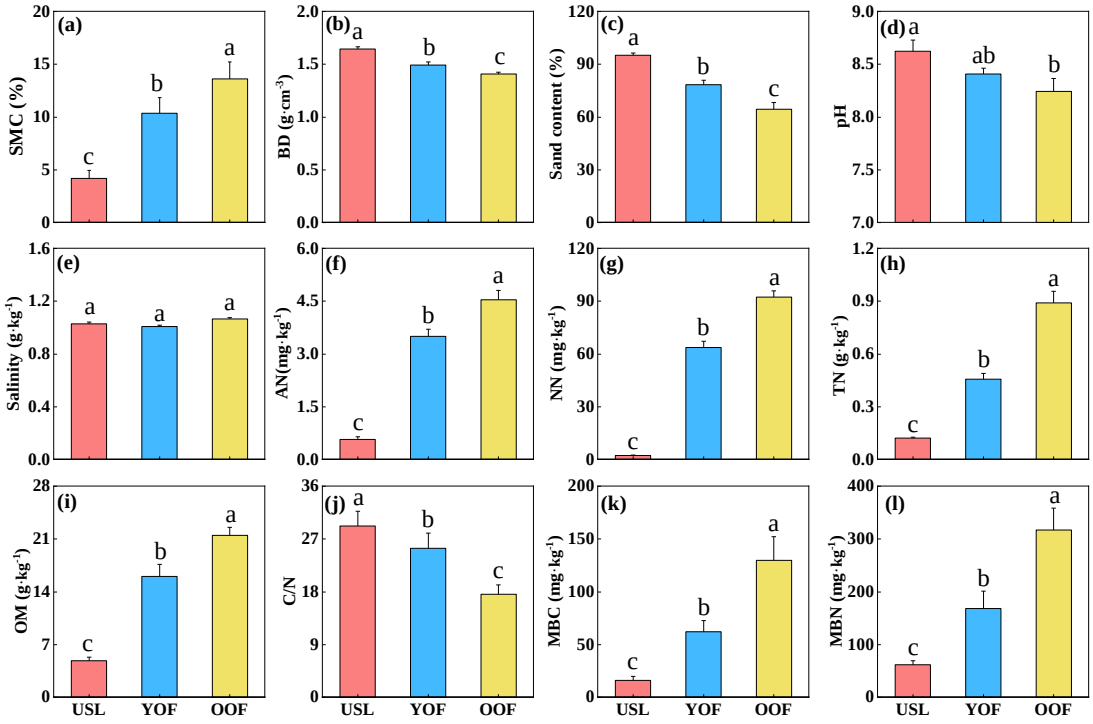

Fig. 1. Differences in soil variables across 3 sites, uncultivated sandy land (USL), young oasis field (YOF), and old oasis field (OOF). Abbreviations: SMC: Soil moisture content. BD: soil bulk density. AN: NH_4^+-N content. NN: NO_3^--N content. TN: total N content. OM: organic matter content. MBN: microbial biomass nitrogen content. MBC: microbial biomass carbon content.

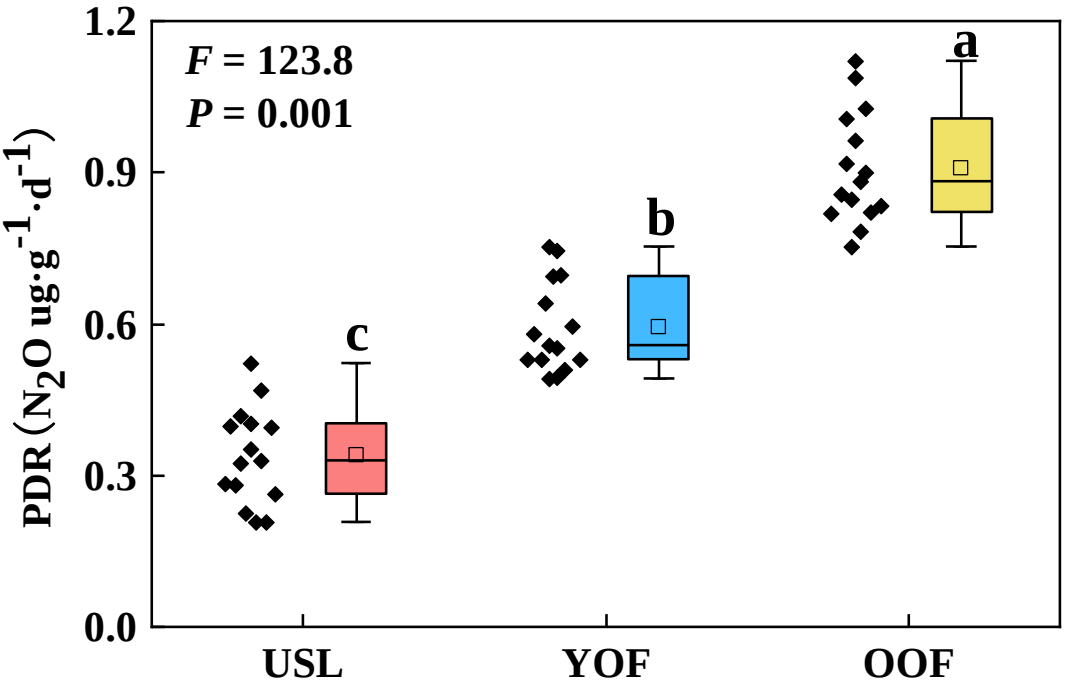

Fig. 2. Potential denitrification rates (PDR) in three sites. USL, uncultivated sandy land; YOF, young oasis field; OOF, old oasis field. Different letters above box plots indicate highly significant differences among sites (P = 0.001); F, Fisher test.

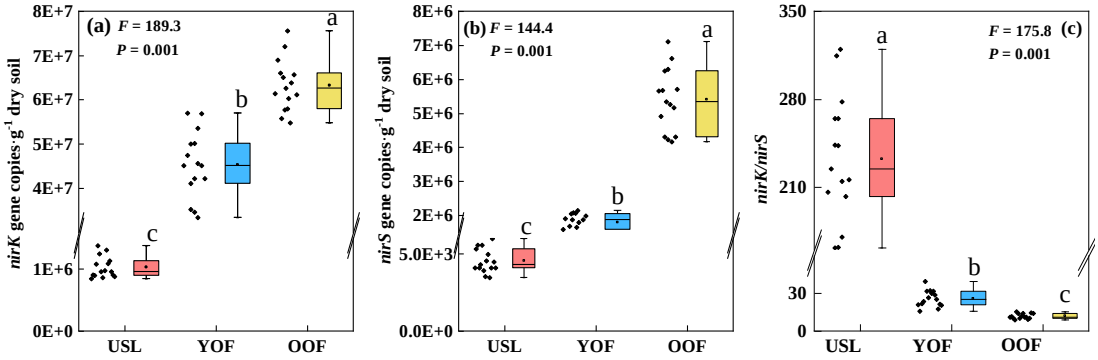

Fig. 3. Absolute abundances of *nirK* (a), *nirS* (b) and *nirK / nirS* ratios (c) across three sites. USL, uncultivated sandy land; YOF, young oasis field; OOF, old oasis field. Different letters above box plots indicate highly significant differences among sites ($P = 0.001$; Fisher test).

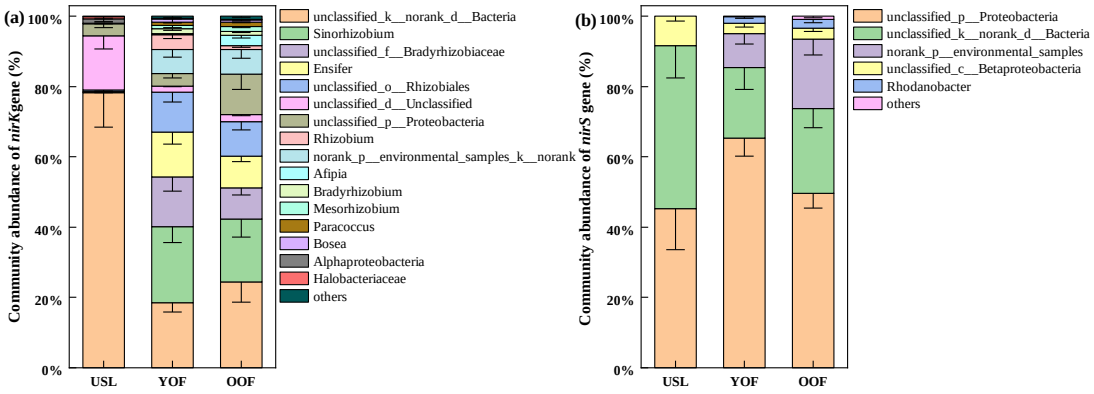

Fig. 4. Genus -level taxonomy of relative abundances of *nirK* (a) and *nirS* (b) functional genes across three sites. Bars represent means of five replicates. USL, uncultivated sandy land; YOF, young oasis field; OOF, old oasis field.

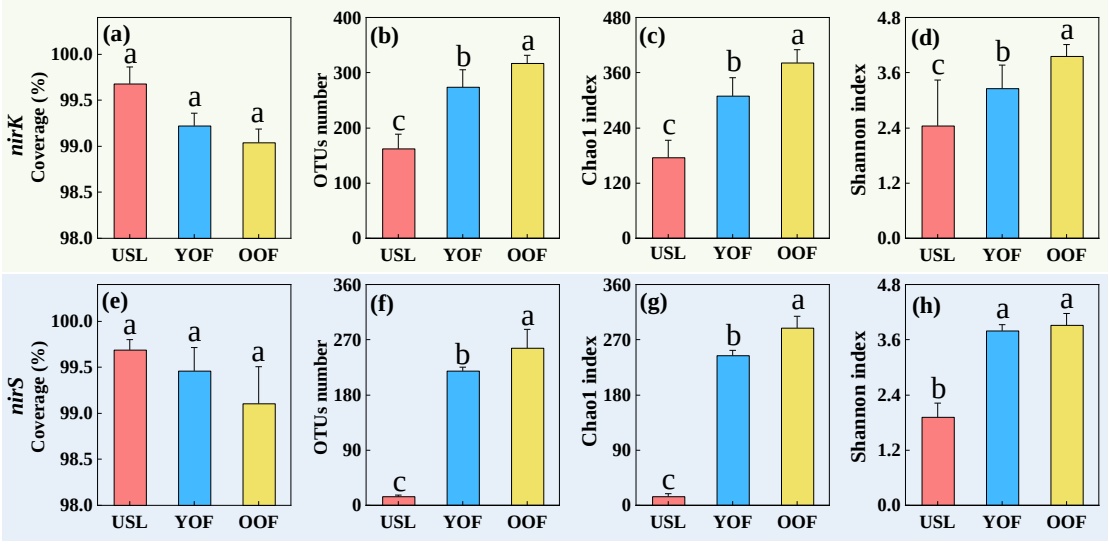

Fig. 5. Coverage, OTUs number, Chao1 index, and Shannon diversity index of *nirK* (a, b, c and d), and *nirS* (e, f g and h) functional genes across uncultivated sandy land (USL), young oasis field (YOF) and old oasis field (OOF). The values given are means ± SD (n=5), different letters indicate significant differences among sampling sites ($P < 0.05$, Fisher's LSD test)

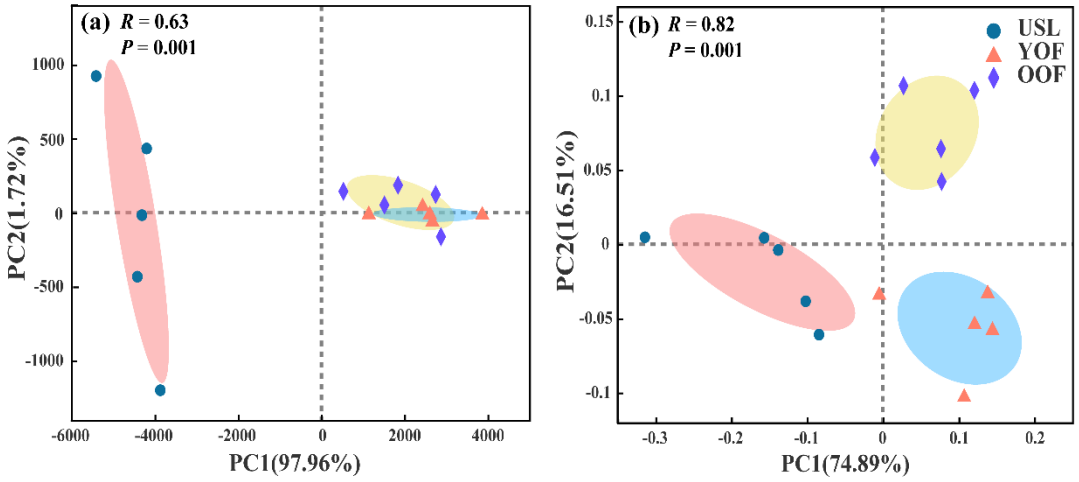

Fig. 6. Principal coordinates analysis (PCoA) (at the phylum level) of the *nirK* genes communities (a) and *nirS* genes communities (b) across uncultivated sandy land (USL; green dots), young oasis field (YOF; orange triangles) and old oasis field (OOF; purple diamonds) (*n*=5). Values at axes 1 and 2 are the percentages that can be explained by the corresponding axis.

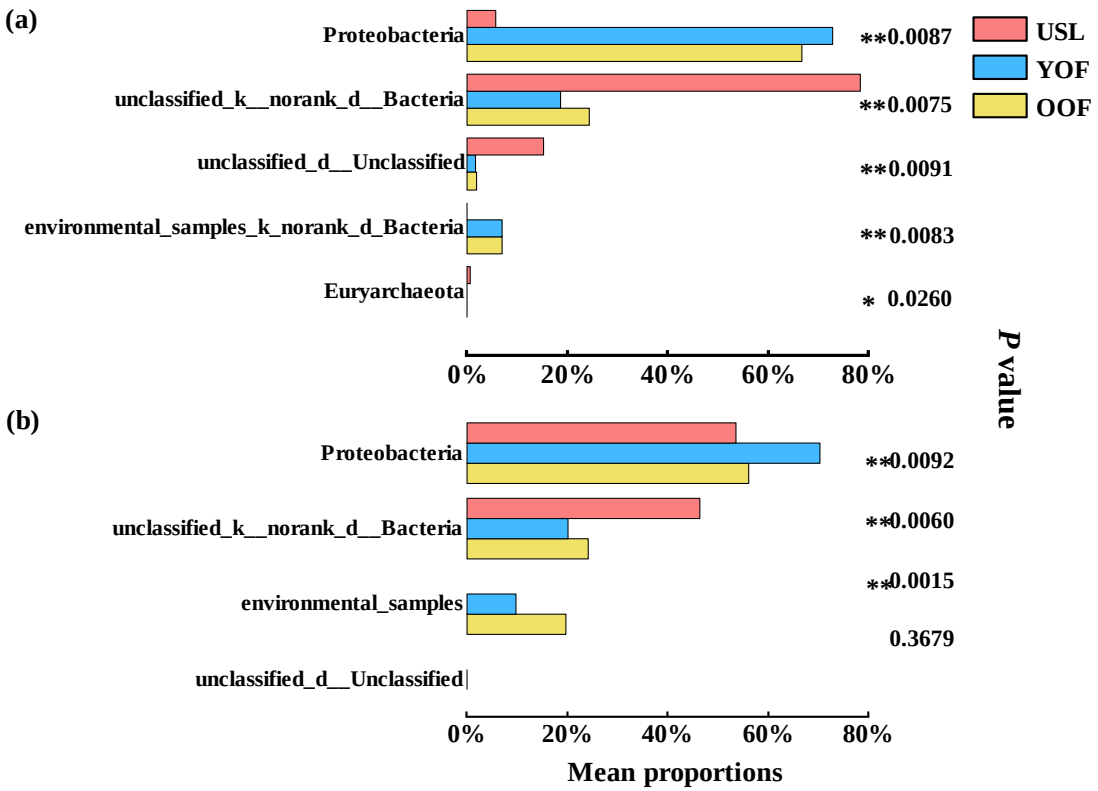

Fig. 7 The Kruskal-Wallis H test of species (at the phylum level) with different abundances of nirK (a), and nirS (b) genes communities across uncultivated sandy land (USL), young oasis field (YOF) and old oasis field (OOF) (n = 5,*P ≤ 0.05, **P ≤ 0.01).

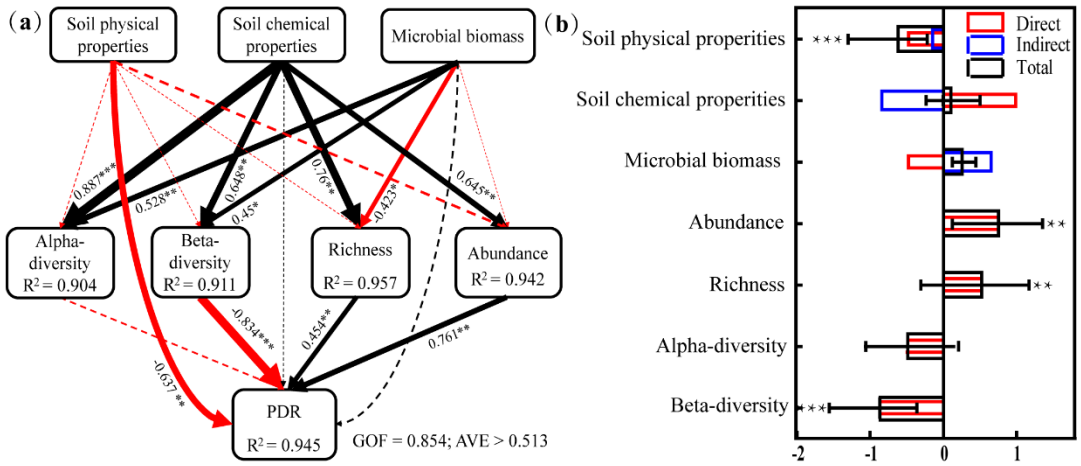

Fig. 8. The partial least squares path model (PLS-PM) and standardized total effect (STE, ±bootstrap 95% confidence interval). Boxes represent latent or observed variables. Larger path coefficients are reflected in arrow width. Black arrows indicate a positive effect; red arrows indicate a negative effect. Solid arrows indicate that the effect was significant; dashed arrows indicate that the effect was not significant. *P < 0.05, **P < 0.01, or ***P < 0.001. GOF is the goodness of fit, which is a measure of the overall prediction. AVE is average variance extracted, which is used to estimate the aggregation validity of the model

Table 1 Primers and thermal cycling conditions for qPCR

Target gene	Primers	Sequence (5´-3´)	Amplicon length (bp)	Cycling conditions	Refs.
nirK	LWC-*nirK*-F	ATCATGGTSCTGCCGCG	471	95 ℃, 60s; 58 ℃, 30s;	Wang et al.
	LWC-*nirK*-R	GCCTCGATCAGRTTGTGGTT		72 ℃, 45s	(2022)
nirS	*nirS*4F	TTCRTCAAGACSCAYCCGAA	322	95 ℃, 60s; 58 ℃, 30s;	Wang et al.
	*nirS*6R	CGTTGAACTTRCCGGT		72 ℃, 45s	(2021)

Table 2 Loading coefficient between observed and latent variables

Latent variables	Observation variables	SPP	SCP	MB	Richness	Abundance	α-diversity	β-diversity	PDR
SPP	SMC	-0.952	0.955	0.914	0.901	0.950	0.8518	0.907	0.895
	BD	0.944	-0.979	-0.922	-0.939	-0.969	-0.908	-0.928	-0.941
	Sand	0.958	-0.962	-0.956	-0.931	-0.954	-0.866	-0.890	-0.965
SCP	pH	0.86	-0.849	-0.793	-0.843	-0.837	-0.786	-0.890	-0.911
	Salt	-0.483	0.412	0.629	0.267	0.378	0.243	0.165	0.565
	AN	-0.949	0.989	0.915	0.765	0.889	0.827	0.7709	0.84
	NN	-0.966	0.947	0.934	0.892	0.977	0.922	0.859	0.923
MB	MBC	-0.922	0.922	0.927	0.821	0.892	0.786	0.805	0.929
	MBN	-0.947	0.92	0.997	0.852	0.907	0.785	0.810	0.931
Richness	*nirK*-OTU	-0.748	0.789	0.733	0.883	0.784	0.871	0.803	0.739
	nirS- OTU	-0.925	0.97	0.856	0.985	0.967	0.947	0.983	0.891
Abundance	*nirK*	-0.957	0.977	0.917	0.959	0.917	0.926	0.955	0.931
	nirS	-0.907	0.902	0.957	0.809	0.885	0.764	0.768	0.939

	nirK-Shannon	-0.68	0.727	0.642	0.775	0.731	0.8839	0.727	0.684
	nirS- Shannon	-0.883	0.934	0.798	0.973	0.938	0.948	0.974	0.827
α-diversity	*nirK*-PC1	-0.878	0.947	0.799	0.964	0.945	0.934	0.996	0.823
	nirS-PC1	-0.859	0.932	0.785	0.966	0.928	0.946	0.989	0.796
PDR	PDR	-0.964	0.94	0.944	0.888	0.932	0.834	0.842	1

SPP: soil physical properties, SCP: soil chemical properties, MB: microbial biomas